

COVID-19 puzzle in China: a serendipitous interplay between transmissibility and social distancing measures

Marko Djordjevic^{1,*,#}, Magdalena Djordjevic^{2,*,#}, Igor Salom², Andjela Rodic¹, Dusan Zigic², Ognjen Milicevic³, Bojana Ilic²

¹Computational Systems Biology Group, Faculty of Biology, University of Belgrade, Serbia

²Institute of Physics Belgrade, University of Belgrade, Serbia

³Department for Medical Statistics and Informatics, Faculty of Medicine, University of Belgrade, Serbia

* Correspondence: dmarko@bio.bg.ac.rs; magda@ipb.ac.rs

Contributed equally to this work.

Abstract:

Drastic difference in the COVID-19 infection and fatality counts, observed between Hubei (Wuhan) and other Mainland China provinces raised public controversies. To address if these data can be consistently understood, we develop a model that takes into account all main qualitative features of the infection progression under suppression measures, while remaining simple enough to estimate the key dynamics parameters. We find that social distancing measures had a large effect in provinces, where moreover higher transmissibility appears to have triggered more effective protection. Hubei is, however, a far outlier with significantly larger transmissibility, but lower protection. Predicted infection attack rate is significantly higher for Hubei, but much lower than necessary for herd immunity. Case Fatality Rate is five times larger in Hubei, but our estimated Infection Fatality Rates are much more uniform/consistent across all provinces. Therefore, interplay of transmissibility, effective protection, and detection efficiency differences may explain apparently drastic count discrepancies.

Introduction

On January 31st The World Health Organization (WHO) classified COVID-19 outbreak as the Public Health Emergency of International concern (1), due to the epidemics in People Republic of China (PRC) that originated in Wuhan (Hubei province) (2). WHO classified the infection spread as a pandemic (3) on March 11th, which followed large secondary outbreaks in Europe, while later US became a new hotspot (4). The imposed restrictions in different countries ranged from mild to severe, with a significant impact on people's lives, and likely notable future economic consequences (3, 5). After unprecedented containment and infection suppression measures, PRC announced the end of the epidemics on March 29th (6).

Progression of the infection in PRC seems highly intriguing, as Hubei (with only 4% of PRC population) shows an order of magnitude larger number of confirmed infection cases (Fig. 1A), and two order of magnitude higher fatalities (Fig. 1B) compared to the *total* sum in all other Mainland China provinces. The epidemics was unfolding well before the Wuhan/Hubei closure (with the reported symptom onset of the first patient on December 1st 2019), and within the period of huge population movement, which started two weeks before January 25th (the Chinese Lunar New Year) (7). As a rough baseline, a modeling study (8) based on the Wuhan infection dynamics, estimated as many as 150,000 confirmed cases per day in

Chongqing alone (due to its large population coupled with intense travel volume with Wuhan) – instead, the actual (reported) peak number for *all* Mainland China outside Hubei was just 831.

Magnitude of the subsequent outbursts in Europe and USA is comparably even more surprising. For example, Ireland, with the population size of 4.9 million (two orders of magnitude smaller than PRC population), as of May 15th has almost two times *more* confirmed infection cases than all Mainland China except Hubei (~24.000 compared to ~13.000) and more than order of magnitude larger number of fatalities (1.506 compared to 116). Such extreme disproportions have created a public media controversy (9-10), where e.g., “The New York Times” reported that the Central Intelligence Agency has been warning the USA administration that China is underreporting their coronavirus cases (11). A political controversy also unfolded, where similar concerns have been publicly expressed by the highest ranking USA, France and UK officials (12).

These allegations were strongly denied by PRC: On May 9th, Chinese Foreign Ministry published a response (13) to different (PRC related) COVID-19 controversies, where points 11 and 12 address allegations that China underreported confirmed case and fatality numbers. The rebuttal quoted a study (14), which concluded that China COVID-19 numbers are in accordance with Banford’s law. Two additional papers (15-16) are also quoted: The first paper shows a good correlation between the case counts in provinces outside Hubei, and outbound Wuhan mobility (tracked through mobile phones) (15) – the correlations are however scale invariant, so this also does not explain the drastic case and fatality count differences after January 23rd in Fig. 1. These two studies also show that Wuhan quarantine set much lower initial conditions (number of detected cases and fatalities on January 23rd) for the infected in other provinces, which is intuitively plausible. However, these initial conditions were still about the same for Hubei and all other provinces (see Fig. 1), while the subsequent (after January 23rd) time evolutions are drastically different.

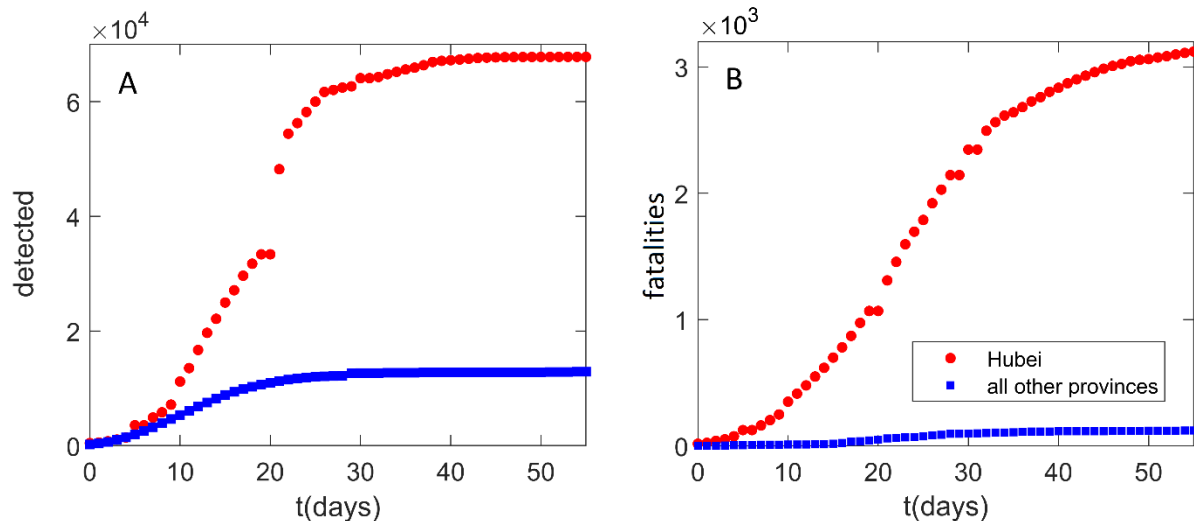


Figure 1: Infection and fatality counts for Hubei vs. all other provinces. Number of A) Confirmed infections, B) Fatality cases. Zero on the horizontal axis corresponds to the time from which the data are taken (January 23rd), which also coincides with the Wuhan closure. Red circles correspond to the observed Hubei counts. Blue squares correspond to the sum of the number of counts for all other provinces. The figure illustrates a puzzling difference in the number of counts between Hubei alone, and the sum of all other mainland China provinces.

In this study we analyze the puzzling differences in dynamics trajectories in Mainland China provinces, which may put strong constraints on the underlying infection progression parameters:

1. What interplay between the transmissibility and the suppression measure effects is responsible for the large difference in the count numbers between Hubei and the rest of PRC?
2. What is the Infected Fatality Rate (IFR, the number of fatalities per *infected* persons) in PRC? Case Fatality Rate (CFR, the number of fatalities per *detected* cases) can be obtained directly from the data, but is highly sensitive to the testing capacity (larger testing coverage leads to lower CFR). IFR is a more fundamental mortality parameter, as it does not depend on the testing coverage, but is however much harder to determine, due to the unknown number of infected cases.
3. What is the infection attack rate (AR), i.e. a fraction of population that got infected (and presumably became resistant afterwards), in Hubei and other provinces? Estimating AR allows understanding risks that the epidemic will reinitiate. As this study is completed, PRC announced that they will assess AR in Wuhan through serology tests on almost entire Wuhan population (17), which will allow a direct comparison with our predictions.

Addressing these questions allows understanding of both different response policies, and inherent risks posed by the pandemics, and will enable future cross-country comparisons.

Model and parameter inference

We developed a model that takes into account all main qualitative features of the infection progression under suppression measures. The model however remains simple enough to estimate the key dynamics parameters, individually for each of the provinces. We opt for a deterministic model, as parameter inference (the central issue of our work) from stochastic models (18-19) is still an open problem (20). The relevant case counts are also well in a commonly considered deterministic range ($> \sim 10$), while the transmission process is not strongly non-linear (see below) – for a linear system, mean of the stochastic trajectories corresponds to the deterministic solution (21).

Classical SIR or SEIR models (or their modifications) were up to now used to predict or explain different features of COVID-19 infection dynamics (16, 22-23). SIR-based models may be used to estimate some aspects of the infection dynamics, but they cannot be used to more realistically infer the infection parameters, due to a large number of latent (exposed) individuals, which (due to latency period) show different dynamics compared to the infected population. We thus modify SEIR model, to take into account social distancing (lockdowns, school and university closures, infection induced behavioral changes), consistent with drastic non-pharmaceutical interventions applied in PRC. Quarantine by detecting (and subsequently containing) some *fraction* of the infected is also explicitly taken into account, which accounts for (presumably) large number of the infected that are not detected (5):

$$dS / dt = -\beta \cdot I \cdot S / N - \alpha \cdot S \quad (1)$$

$$dE / dt = \beta \cdot I \cdot S / N - \sigma \cdot E \quad (2)$$

$$dI / dt = \sigma \cdot E - \gamma \cdot I - \varepsilon \cdot \delta \cdot I \quad (3)$$

$$dD / dt = \varepsilon \cdot \delta \cdot I - h \cdot D - m \cdot D \quad (4)$$

$$dH / dt = h \cdot D \quad (5)$$

$$dF / dt = m \cdot D \quad (6)$$

In the above equations S, E, I, D, H, F, N are, respectively: susceptible, exposed, infected, active detected, healed (recovered), fatalities and the total population number. The parameter notation is the following: β -

the infection rate in a fully susceptible population; α - the protection rate, i.e., the rate with which the population moves from susceptible to protected category, quantifying the impact of the social protection measures. The protection rate α is taken as 0 before t_0 (the onset of social measures), and constant afterwards; σ - inverse of the latency period; γ - inverse of the infectious period; δ - inverse of the period of the infected detection/diagnosis; ε - the detection efficiency quantifying the fraction of diagnosed infected population; h - the recovery rate; m - the mortality rate.

In Eq. (1), the susceptible pool is depleted due to both the infection process, and the social distancing measures - moving the susceptible to the protected compartment. Alternatively, a frequently used approach is to account for interventions by modifying β in some assumed form (e.g., with step-wise constant (16) or exponential dependence (24)), through which a phenomenological law is however introduced in otherwise mechanistic (SIR or SEIR) model. We instead introduced social distancing consistent with the SEIR compartmental structure, so that susceptible move to the protected category with rate α . The nonlinearity appears only through the “infection” ($\beta \cdot S \cdot I$)/ N term, so the system is not strongly non-linear (see above). In Eq. (2), the latent population increases due to the infection events, and decreases due to a delayed transition to the infected with rate σ . In Eq. (3), the infected population is increased due to this transition, removed with rate γ , or detected (and isolated/quarantined) with rate $\varepsilon \cdot \delta$. Eq. (4) describes the dynamics of active detected cases, which increase due to detection of the infected, or decrease due to the recovery or fatalities. Eqs. (5) and (6) follow directly from Eq. (4). Note that the dynamics of the protected $dP/dt = \alpha S$, and the resistant $dR/dt = \gamma I$ compartments is not explicitly included in Eqs. (1) - (6), as it does not impact the observable quantities (D, H, F). The corresponding conservation law is $S+E+I+D+H+F+P+R=N$.

The main difficulty in parameter inference is that healing and mortality rates (h and m) are time-dependent, i.e. they, respectively, significantly increase and decrease with time – this can be directly obtained from Eqs. (5) and (6). Consequently, instead of the active detected cases D (which depend on time-dependent h and m rates), we propose as the main observable the total number of detected cases $D_t = D + H + F$, i.e. the sum of active cases, recovered cases and fatalities:

$$\frac{dD_t}{dt} = \varepsilon \cdot \delta \cdot I, \quad (7)$$

where this equation substitutes Eqs. (4) - (6), conveniently removing the rates h and m from our analysis. We further denote our model as $\varepsilon\alpha$ -SEIR, where $\varepsilon\alpha$ denotes that it takes into account not only the basic (unsuppressed) infection dynamics, but also the effective social distancing (through α) and joint quarantine/sampling processes (through ε), which also sets the scale between the “iceberg” (latent and infected) and its “tip” (detected) – with the translocated tip, due to inherent delays in the model (e.g., latency period).

For parameter estimation, Eq. (3) allows separating the social distancing measures ($-\alpha \cdot S$ term in Eq. (1)) from sampling the infected to the protected compartment ($\varepsilon \cdot \delta \cdot I$ in Eq. (4)), through the resulting basic reproduction rate $R_{0,\text{free}} = \beta/(\gamma + \varepsilon \cdot \delta)$. Notation $R_{0,\text{free}}$ is in accordance with (22) (a SIR-based study taking into account social distancing measures), and a definition where R_0 corresponds to completely susceptible population in the absence of social distancing measures (in a completely naive population) (25-26). $R_{0,e}$ from (22) can be recovered following (24), $R_{0,e} = \int_0^\infty \beta S(t)/N \exp(-\gamma t) dt$, under assumptions of sufficiently strong α and small t_0 (immediately effective measures), so that from Eq. (1) $S(t) \sim \exp(-\alpha t)$. $R_{0,e}$ corresponds to another definition of R_0 , which does not require the absence of social distancing

measures (i.e. only non-resistant population). The discussion above explains the empirical observation that R_0 for PRC reported in the literature shows much variation, from 1.4 (27) to recently reported 5.7 (28), as it is not only model (see the integral above), but also definition-dependent. We further adopt $R_0 \equiv R_{0,free}$, in line with the goal of our work, as it allows separating the transmissibility influenced by biological, climate and sociodemographic qualities (R_0) from interventions increasing social distancing (quantified by α and t_0). In addition to R_0 , α and t_0 , two initial conditions (I_0 and E_0), and the detection efficiency ε , are unknown and may differ between the provinces. σ and γ characterize the fundamental infection processes, not expected to change from one province to another, and have consistent mean values between independent studies ($\gamma = 0.4 \text{ days}^{-1}$, $\sigma = 0.2 \text{ days}^{-1}$) (18, 29).

$\varepsilon\alpha$ -SEIR was numerically solved by Runge-Kutta method (30) for each parameter combinations. Parameter values were inferred by exhaustive search over a wide parameter range, to avoid reaching local minimum of the objective function (R^2). To infer the unknown parameters, we fit (by minimizing R^2) $\varepsilon\alpha$ -SEIR to the observed total number of detected D_t for each province. How different properties of D_t curve determine the unknown parameters? Early in the infection, almost the entire population is susceptible ($S \approx N$), so Eqs. (2) and (3) become linear, and decoupled from the rest of the system. This sets the ratio of I_0 to E_0 , through the eigenvector components with the positive eigenvalues of the Jacobian. Similarly, β is set by the initial slope of $\log(D_t)$ curve. From Eq. (7) one can see that the product of I_0 and $\varepsilon \cdot \delta$ is set by dD_t/dt at the initial time ($t=0$). Later dynamics of the D_t curve is determined by the combination $t_\alpha = t_0 + 1/\alpha$ (which we denote as protection time), setting the time at which $\sim 1/2$ of the population moves to the protected category. We also numerically checked this, i.e. t_0 can be lowered at the expense of increasing $1/\alpha$, without affecting the fit quality. Two independent parameters (I_0 and t_α) have to be determined from the late infection dynamics. As social distancing depletes S , D_t curve grows subexponentially, which may be quantified phenomenologically, e.g., through generalized-growth model, and the related growth parameter (24), which sets t_α . D_t curve saturates when the infected are depleted, so the saturation time depends on the scale (height) of the infected curve, which sets I_0 .

Over-fitting is consequently not expected, as the same number of characteristic dynamics features is at least equal to the number of fit parameters. The late dynamics may however be less sensitive to I_0 than to t_α (which directly relates to the dominant subexponential growth of D_t curve). We observed this numerically, where I_0 can sometimes be decreased compared to the best fit value, without noticeably affecting the fit quality. We therefore checked this specifically for each province, and where possible (few provinces), we chose the lowest I_0 value that still leads to a comparably good fit. This allows us to obtain the most conservative (i.e., as high as consistent with the data) IFR estimate, as the reported number of fatalities for all PRC provinces (except Hubei) is surprisingly low.

Errors for the inferred parameters were estimated through Monte-Carlo simulations (31), individually for each province with assumption that count numbers follow Poisson distribution. Monte-Carlo simulations were found as the only reliable estimate of the fit parameter uncertainties for non-linear fit (32), where in our case a closed form expression is moreover not available. P values related with comparison of the calculated/reported quantities are estimated by t -test.

Results

We used $\varepsilon\alpha$ -SEIR with the parameter inference described above, to analyze all Mainland China provinces, with the exception of Tibet, where D_t counts have been very low (below 17). Parameters were estimated

separately for each of the 30 provinces. In Fig. 2A and B, we show that our model can robustly explain the observed D_t , in the cases of large outbreak (Hubei on Fig. 2A), as well as for all other provinces, where D_t is in the range from intermediate (e.g., Guangdong) to low (e.g., Inner Mongolia). Provinces in Fig. 2B were selected to cover the entire range of observed D_t (from lower to higher counts), while equally good fits were obtained for all other provinces, which were all included in the further analysis. Our method is also robust with respect to data perturbations (which might be frequent), e.g., in the case of Hubei (Wuhan), a large number of counts was added on Feb. 12th, based on clinical diagnosis (CT scan) (2), which is apparent as a discontinuity in observed D_t in Fig. 2A. The model however interpolates this discontinuity, finding a reasonable description of the overall data.

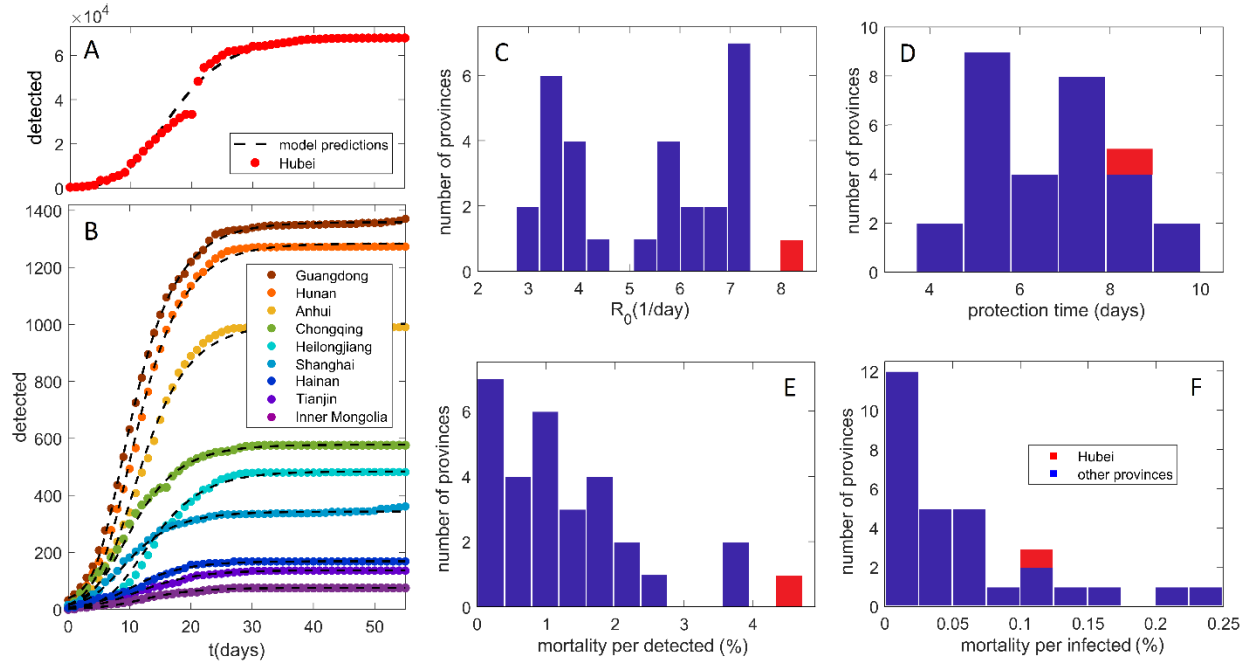


Figure 2: Model predictions: comparison with data and key parameter estimates. Predictions (compared to data) of confirmed infection counts and for A) Hubei, B) other Mainland China provinces. The observed counts are shown by dots, and our model predictions by dashed curves. Names of the provinces are indicated in the legend, with provinces selected to cover the full range of the observed total detected counts. The distribution with respect to provinces of C) the basic reproduction number R_0 , D) the protection time t_a . E) Case Fatality Rate - proportion of fatalities out of total detected cases. F) Infected Fatality Rate - fatalities per total infected. The values for Hubei are indicated by the red bars.

We back propagated the dynamics inferred for Hubei, to estimate that January 5th (± 4 days) was the onset of the infection exponential growth in the population (not to be confused with the appearance of first infections, which likely happened in December (2)). This agrees well with (2) (cf. Fig. 3A), which tracked cases according to their symptom onset (shifted for ~ 12 days with respect to detection/diagnosis, cf. Fig. 3B), and coincides with WHO reports on social media that there is a cluster of pneumonia cases – with no deaths – in Wuhan (33). Since our analysis does not directly use any information prior to January 23rd, this agreement provides confidence in our I_0 (see above) estimate, on which depend our estimates of IFR and AFR below.

Key parameters inferred from our analysis are summarized in Fig. 2C-F, with individual results and errors for all the provinces shown in Supplement. Fig. 2C shows the distribution of transmissibility R_0 . Note that

R_0 might depend on demographic (population density, etc.) and climate factors (temperature, humidity...), which are not controllable, but is unrelated to the applied social distancing measures, which are prone to intervention (see the discussion on above). Obtained average R_0 for provinces outside of Hubei is 5.3 ± 0.3 , in a reasonable agreement with a recent estimate (≈ 5.7). Furthermore, we observe that R_0 for Hubei is a far outlier with R_0 value of 8.2 ± 0.4 , which is notably larger than for other provinces with $p \sim 10^{-11}$. This then strongly suggests that demographic and climate factors that determine R_0 , played a decisive role in a large outbreak in Hubei vs. other provinces, which we further address below.

Distribution of protection time t_α for the provinces is shown in Fig. 2D, with the value for Hubei indicated in red. The mean for other provinces is 6.6 ± 0.2 days. That is, we observe that the suppression measures were efficiently implemented, with $\sim 1/2$ of the population moving to the protected category within a week from Wuhan closure. The protection time for Hubei of 8.3 ± 0.2 days was noticeably longer, which is statistically significant at $p \sim 10^{-11}$ level. The estimated less efficient protection in the case of Hubei may also be an important contributing factor in the surprising difference in Hubei vs. other provinces, which we further investigate below.

CFR distribution, based on the fatality numbers reported for Hubei and other provinces is shown in Fig. 2E. These numbers are not based on the model predictions, i.e. can be straightforwardly obtained by dividing the total number of fatalities with the total number of detected cases. CFR for other provinces with a mean of $1.2 \pm 0.4\%$, is significantly smaller compared to CFR for Hubei, which was 4.6% before the correction on April 17th, and 6.5% after the correction (with 1290 fatalities added to Wuhan). This drastic difference in CFR between Hubei and other provinces further accentuates the differences noted in Fig. 1.

IFR distribution, which provides a much less biased measure of the infection mortality, is shown in Fig. 2F. In distinction to CFR, estimated IFR shows a much smaller difference between Hubei ($0.15\% \pm 0.09\%$) and other provinces ($0.056 \pm 0.007\%$). Therefore, while Hubei is a clear outlier with respect to CFR, we observe similar IFR values for all PRC provinces, where few provinces have even higher IFR than Hubei. The ratio of IFR to CFR equals the fraction of all infected that got detected (*detection coverage*). We estimate that the mean detection coverage for all provinces except Hubei is higher than detection coverage for Hubei ($4.5 \pm 0.9\%$ vs. $2 \pm 2\%$). This difference is responsible for decrease by a factor of two from CFR to IFR for Hubei, compared to the other provinces, and consequently for more uniform mortality estimates at IFR level. Xinjiang (Uyghur Autonomous Region) has the highest IFR of $0.25 \pm 0.09\%$, so that Hubei is not an outlier anymore.

In Fig. 3A, two key infection progression parameters are plotted against each other: protection time t_α vs. transmissibility R_0 . Unexpectedly, there is a high negative correlation, with Pearson correlation coefficient $R = -0.70$, which is statistically highly significant $p \sim 10^{-5}$. Note that these two are *a priori* unrelated as $R_0 \equiv R_{0,free}$ (see above). Even for $R_{0,e}$, stronger social distancing measures would decrease it (see above), leading to a tendency to be positively correlated with t_α , oppositely from the strong negative correlation in Fig. 3A. Therefore, higher transmissibility is related with a shorter protection time (larger effect of the suppression measures). Intuitively, this could be understood as a negative feedback loop, where larger R_0 leads to steeper initial growth in the infected numbers, but which may subsequently elicit stronger measures.

We however see that Hubei (marked in red) is a far outlier. That is, while there is a clear tendency that higher R_0 leads to higher suppression, Hubei is located in the upper right quadrant, characterized by both high transmissibility (R_0) and relatively low suppression effect (high t_α).

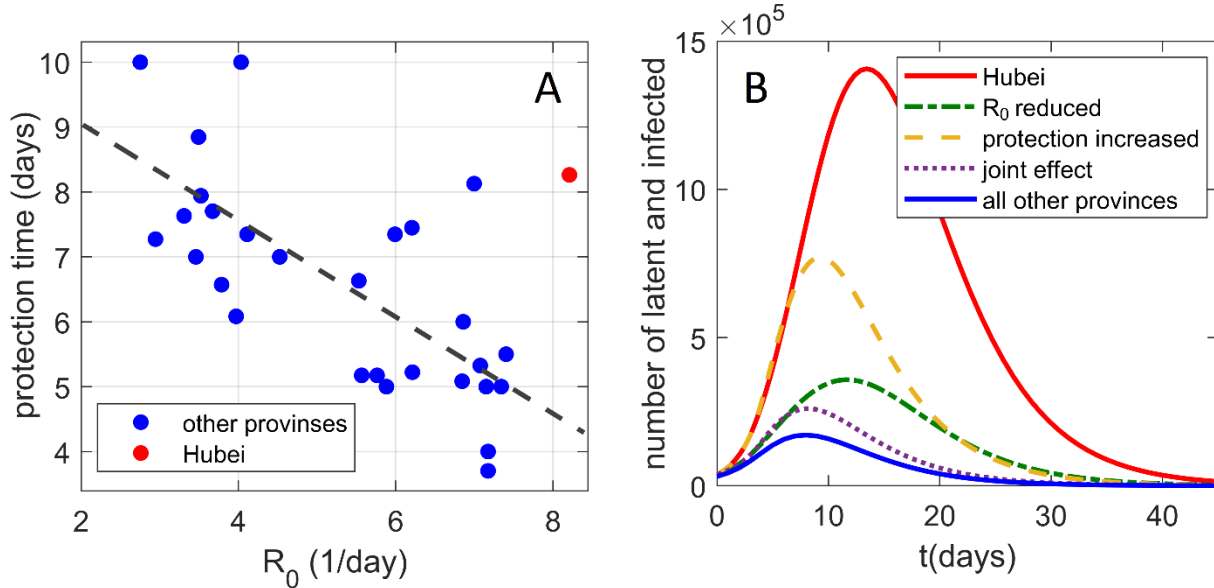


Figure 3: Interplay of transmissibility and effective social distancing. A) The correlation plot of t_a vs. R_0 for all provinces, where the point corresponding to Hubei is marked in red. B) The effect (on the Hubei dynamics of infected and latent cases) of reducing R_0 and t_a to the mean values of other PRC provinces. Both the unperturbed Hubei dynamics and the sum of infected and latent cases for all other provinces is included as a reference.

Two main properties of the Hubei outburst are therefore high R_0 and higher t_a compared to other provinces. In Fig. 3B, we investigate how these two properties separately affect the Wuhan outburst for latent and infected cases, where unperturbed Hubei dynamics is shown by the red full curve. We first reduce only R_0 from the Hubei value, to the mean value for all other provinces (the dash-dotted green curve). We see that reducing R_0 substantially reduces the peak of the curve, though it still remains wide. Next, instead of decreasing R_0 , we decrease the protection t_a to the mean value for all other provinces (dashed orange curve). While reducing t_a also significantly lowers the peak of the curve, its main effect is in narrowing the curve, i.e. reducing the outburst time. Finally, when R_0 and t_a are jointly reduced, we obtain the (dotted purple) curve that is both significantly lower and narrower than the original Hubei progression. This curve comes quite close to the curve that presents the sum of all other provinces (full blue curve) - the dotted curve remains somewhat above this sum, mainly because the initial number of latent and infected cases is somewhat higher for Hubei compared to the sum of all other provinces. The synergy between the transmissibility and the suppression measures, will be further discussed below.

Discussion and summary

The infection progression in PRC has led to a puzzling difference in the number of counts observed between Hubei and other Mainland China provinces, which has in part created first public media, and then high-level political controversy (see Introduction). On April 17th, PRC has also revised their numbers, substantially increasing (for $\sim 50\%$) its fatality count, which our analysis takes into account. A naive explanation of the puzzle might be that closing Wuhan prevented the influx of the infected to other Chinese provinces. It was however previously shown that, at the start of the travel ban, most Chinese cities had already received many infected travelers (34), which is also consistent with the fact that the initial number of detected (and our estimates of the infected) cases, were similar in Wuhan compared to the sum in all other provinces.

To resolve this puzzle, we here formulated $\varepsilon\alpha$ -SEIR model and corresponding parameter inference procedure. $\varepsilon\alpha$ -SEIR (as well as other SIR or SEIR based models) could be further extended, by including a larger number of compartments, e.g., to stratify population according to their demographic properties (which in the limit leads to individual-based models). This would enable detailed projections from the model, e.g., effects of preferentially protecting certain age group. However, the number of parameters increases as a square of the number of compartments (24), which may be a major obstacle in the context of parameter inference. For example, in an individual-based model, parameters were *jointly* fitted to fatality counts from 11 different countries (35), which is not feasible in our case, where parameters have to be estimated *individually* for each PRC province. Consequently, our approach is well suited for the problem considered, where population average parameters are to be separately estimated from individual time-series data.

We here obtained that Hubei was an outlier with respect to two key infection progression parameters: having significantly larger R_0 , and a longer time needed to move a sizable fraction of the population from susceptible to protected category. It is interesting that the initial origin of the epidemic (Hubei) has also a significantly larger R_0 compared to all other provinces, as in principle these two do not have to be related. While stricter measures were formally introduced in Hubei, the initial phase of the outburst put a large strain on the system, arguably leading to less effective measures compared to other provinces (13).

The fact that the initial epidemic in Hubei was not followed by similar outbursts in the rest of PRC may be understood as a serendipitous interplay of the two factors noted above. While both smaller R_0 and lower half-protection time (more efficient measures) significantly suppress the infection curve, their effect is also qualitatively different. While lowering R_0 more significantly suppresses the peak, decreasing the half-protection time significantly reduces the outburst duration. Consequently, the synergy of these two effects appears to lead to drastically suppressed infection dynamics in other Mainland China provinces compared to Hubei. The number of detected (diagnosed) cases in entire PRC is therefore, though unintuitive, well consistent with the model, and may be explained by a seemingly reasonable combination of circumstances.

The fatality rates, however, appear to be more controversial. As a partial explanation, we here find a significant change in relative differences between CFR and IFR. While CFR is more than five times larger for Hubei, the numbers appear much more self-consistent at the level of IFR, with Hubei comparable to other PRC provinces. We show that this is due to smaller testing coverage in Hubei, which appears to be consistent with known testing capacities (10000 tests per day in Hubei, vs. 40000 tests per day in all other provinces with significantly smaller total infection cases), and with WHO report on contact tracing in PRC provinces (36). Despite that IFR appears consistent between the provinces, it does look unusual that for as many as 13 provinces (with otherwise huge population) there have been no reported COVID-19 fatalities. This suggests that a careful review (as done for Wuhan) might be needed, since some of the fatalities might be misclassified. However, even this is unlikely to significantly change our overall result of relatively low IFR coming from PRC epidemics. Ethnicity/racial factors might also contribute to low IFR in PRC, as we inferred the highest IFR (noticeably surpassing that of Hubei, even with the most recent revision) for Xinjiang province. Uyghur majority in Xinjiang have been genetically linked with mixed European/ West Asian (being dominant) and East Asian ancestry (37), which in that respect might better reflect mortality in European and US hotspots. Overall, however, our study infers that COVID-19 in PRC has been a highly contagious disease, with transmissibility in-between those of influenza ($R_0 \sim 1-2$) (38) and measles ($R_0 \sim 12-18$) (39), and with IFR comparable to these two diseases (36, 40), but with almost completely naive

population even after the first infection wave (see below). Consistency of these results with those in other countries still remains to be carefully studied and understood.

Finally, our analysis also indicates a very low overall infection attack rate (AR). That is, we obtained that a fraction of PRC population that got infected (and presumably resistant), is just $5\pm 3\%$ for Hubei, and about two orders of magnitude lower for other provinces. If confirmed through serology tests (see above), the obtained low AR (i.e. the associated low fraction of presumably resistant population) may be concerning in a longer term, since what really quelled the infection was rapidly moving the population from susceptible to protected category through drastic social distancing measures. These measures forced the infection curve to an essentially unstable fixed point, as stochastic simulations showed that as few as 5 individuals are sufficient for the infection onset (41).

Therefore, as the measures are abolished, and if SARS-CoV-2 inherent virulence does not weaken (by mutations, changing weather conditions, etc.), the infection may reinitiate. There might already be signs of this for China, since as of May 11th new domestic clusters of COVID-19 cases were reported in Wuhan and Jilin province (42), where Shulan (Jilin province) declared martial law, went into lockdown, and temporarily shut all public places (43). There are also early indications that our estimates of low AR for China, may also be globally representative, e.g., based on a small scale epidemiological study, it was recently concluded that ~1.8 million people in Germany (~2% of the population) might have been infected (44). If so, and given the obtained high transmissibility of COVID-19, second wave infections might be expected globally, as a number of nations begin easing lockdown.

References

1. *Novel Coronavirus (2019-nCoV): Situation Report - 11 (31 January 2020)* (World Health Organization, Geneva, Switzerland, 2020).
2. The Novel Coronavirus Pneumonia Emergency Response Epidemiology Team, The epidemiological characteristics of an outbreak of 2019 novel coronavirus diseases (COVID-19)—China, 2020. *China CDC Weekly* **2**, 113-122 (2020).
3. *Coronavirus disease 2019 (COVID-19): situation report - 70* (World Health Organization, Geneva, Switzerland, 2020).
4. E. Dong, H. Du, L. Gardner, An interactive web-based dashboard to track COVID-19 in real time. *The Lancet Infectious Diseases* **20**, 533-534 (2020).
5. W. H. Organization, *Coronavirus disease 2019 (COVID-19) situation reports*, (<https://www.who.int/emergencies/diseases/novel-coronavirus-2019/situation>).
6. China publishes timeline on COVID-19 information sharing, int'l cooperation. *Xinhua*. Retrieved from http://www.xinhuanet.com/english/2020-04/06/c_138951662.htm (2020, April 6).
7. S. Chen, J. Yang, W. Yang, C. Wang, T. Bärnighausen, COVID-19 control in China during mass population movements at New Year. *The Lancet* **395**, 764-766 (2020).
8. V. Ting, China coronavirus: Hong Kong medical experts call for 'draconian' measures in city as research estimates there are already 44,000 cases in Wuhan. *South China Morning Post*. Retrieved from <https://www.scmp.com/news/hong-kong/health-environment/article/3047813/china-coronavirus-hong-kong-medical-experts-call> (2020, January 27).
9. C. Campbell, A. Gunia, China Says It's Beating Coronavirus. But Can We Believe Its Numbers? *TIME*. Retrieved from <https://time.com/5813628/china-coronavirus-statistics-wuhan/> (2020, April 1).

10. Coronavirus: Why China's claims of success raise eyebrows. *BBC*. Retrieved from <https://www.bbc.com/news/world-asia-china-52194356> (2020, April 7).
11. J. E. Barnes, C.I.A. Hunts for Authentic Virus Totals in China, Dismissing Government Tallies. *The New York Times*. Retrieved from <https://www.nytimes.com/2020/04/02/us/politics/cia-coronavirus-china.html?searchResultPosition=1> (2020, April 16).
12. S. McDonnell, Coronavirus: China outbreak city Wuhan raises death toll by 50%. *BBC*. Retrieved from <https://www.bbc.com/news/world-asia-china-52321529> (2020, April 17).
13. Reality Check of US Allegations Against China on COVID-19. *Xinhua*. Retrieved from http://www.xinhuanet.com/english/2020-05/10/c_139044103.htm (2020, May 10).
14. C. Koch, K. Okamura, Benford's Law and COVID-19 Reporting. Available at SSRN: <https://ssrn.com/abstract=3586413> or <http://dx.doi.org/10.2139/ssrn.3586413> (2020, April 28).
15. J. S. Jia, X. Lu, Y. Yuan, G. Xu, J. Jia, N. A. Christakis, Population flow drives spatio-temporal distribution of COVID-19 in China. *Nature*, 1-11 (2020).
16. H. Tian, Y. Liu, Y. Li, C.-H. Wu, B. Chen, M. U. Kraemer, B. Li, J. Cai, B. Xu, Q. Yang, An investigation of transmission control measures during the first 50 days of the COVID-19 epidemic in China. *Science* **368**, 638-642 (2020).
17. V. Ni, Coronavirus: Can China test all of Wuhan in only 10 days? *BBC*. Retrieved from <https://www.bbc.com/news/world-asia-china-52651651> (2020, May 15).
18. A. J. Kucharski, T. W. Russell, C. Diamond, Y. Liu, J. Edmunds, S. Funk, R. M. Eggo, F. Sun, M. Jit, J. D. Munday, Early dynamics of transmission and control of COVID-19: a mathematical modelling study. *The Lancet Infectious Diseases* **20**, 553-558 (2020).
19. R. Verity, L. C. Okell, I. Dorigatti, P. Winskill, C. Whittaker, N. Imai, G. Cuomo-Dannenburg, H. Thompson, P. G. T. Walker, H. Fu, A. Dighe, J. T. Griffin, M. Baguelin, S. Bhatia, A. Boonyasiri, A. Cori, Z. Cucunubá, R. FitzJohn, K. Gaythorpe, W. Green, A. Hamlet, W. Hinsley, D. Laydon, G. Nedjati-Gilani, S. Riley, S. van Elsland, E. Volz, H. Wang, Y. Wang, X. Xi, C. A. Donnelly, A. C. Ghani, N. M. Ferguson, Estimates of the severity of coronavirus disease 2019: a model-based analysis. *The Lancet Infectious diseases*. 2020 (10.1016/s1473-3099(20)30243-7).
20. D. J. Wilkinson, *Stochastic modelling for systems biology*. (Chapman and Hall/CRC, London, ed. 3, 2018).
21. C. Gadgil, C. H. Lee, H. G. Othmer, A stochastic analysis of first-order reaction networks. *Bulletin of mathematical biology* **67**, 901-946 (2005).
22. B. F. Maier, D. Brockmann, Effective containment explains subexponential growth in recent confirmed COVID-19 cases in China. *Science* **368**, 742-746 (2020).
23. J. S. Weitz, S. J. Beckett, A. R. Coenen, D. Demory, M. Dominguez-Mirazo, J. Dushoff, C.-Y. Leung, G. Li, A. Măgălie, S. W. Park, Modeling shield immunity to reduce COVID-19 epidemic spread. *Nature Medicine*. 2020 (10.1038/s41591-020-0895-3).
24. G. Chowell, L. Sattenspiel, S. Bansal, C. Viboud, Mathematical models to characterize early epidemic growth: A review. *Physics of life reviews* **18**, 66-97 (2016).
25. S. Eubank, I. Eckstrand, B. Lewis, S. Venkatramanan, M. Marathe, C. Barrett, Commentary on Ferguson, et al., "Impact of Non-pharmaceutical Interventions (NPIs) to Reduce COVID-19 Mortality and Healthcare Demand". *Bulletin of Mathematical Biology* **82**, 1-7 (2020).
26. Y. M. Bar-On, A. I. Flamholz, R. Phillips, R. Milo, SARS-CoV-2 (COVID-19) by the numbers. *arXiv preprint*, arXiv:2003.12886 (2020).

27. J. T. Wu, K. Leung, M. Bushman, N. Kishore, R. Niehus, P. M. de Salazar, B. J. Cowling, M. Lipsitch, G. M. Leung, Estimating clinical severity of COVID-19 from the transmission dynamics in Wuhan, China. *Nature Medicine* **26**, 506-510 (2020).
28. S. Sanche, Y. T. Lin, C. Xu, E. Romero-Severson, N. Hengartner, R. Ke, High Contagiousness and Rapid Spread of Severe Acute Respiratory Syndrome Coronavirus 2. *Emerging infectious diseases*. 2020 (10.3201/eid2607.200282).
29. Q. Li, X. Guan, P. Wu, X. Wang, L. Zhou, Y. Tong, R. Ren, K. S. Leung, E. H. Lau, J. Y. Wong, Early transmission dynamics in Wuhan, China, of novel coronavirus–infected pneumonia. *New England Journal of Medicine* **382**, 1199-1207 (2020).
30. J. R. Dormand, P. J. Prince, A family of embedded Runge-Kutta formulae. *Journal of computational and applied mathematics* **6**, 19-26 (1980).
31. W. H. Press, B. P. Flannery, S. A. Teukolsky, W. T. Vetterling, *Numerical recipes: The art of scientific computing*. (Cambridge University Press, Cambridge, 1986).
32. R. W. Cunningham, Comparison of three methods for determining fit parameter uncertainties for the Marquardt Compromise. *Computers in Physics* **7**, 570-576 (1993).
33. *WHO Timeline - COVID-19* (World Health Organization, Geneva, Switzerland, 2020).
34. M. Chinazzi, J. T. Davis, M. Ajelli, C. Gioannini, M. Litvinova, S. Merler, A. P. y Piontti, K. Mu, L. Rossi, K. Sun, The effect of travel restrictions on the spread of the 2019 novel coronavirus (COVID-19) outbreak. *Science* **368**, 395-400 (2020).
35. S. Flaxman, S. Mishra, A. Gandy, H. J. T. Unwin, H. Coupland, T. A. Mellan, H. Zhu, T. Berah, J. W. Eaton, P. N. P. Guzman, N. Schmit, L. Callizo, K. E. C. Ainslie, M. Baguelin, I. Blake, A. Boonyasiri, O. Boyd, L. Cattarino, C. Ciavarella, L. Cooper, Z. Cucunubá, G. Cuomo-Dannenburg, A. Dighe, B. Djaafara, I. Dorigatti, S. van Elsland, R. FitzJohn, H. Fu, K. Gaythorpe, L. Geidelberg, N. Grassly, W. Green, T. Hallett, A. Hamlet, W. Hinsley, B. Jeffrey, D. Jorgensen, E. Knock, D. Laydon, G. Nedjati-Gilani, P. Nouvellet, K. Parag, I. Siveroni, H. Thompson, R. Verity, E. Volz, P. G. Walker, C. Walters, H. Wang, Y. Wang, O. Watson, C. Whittaker, P. Winskill, X. Xi, A. Ghani, C. A. Donnelly, S. Riley, L. C. Okell, M. A. C. Vollmer, N. M. Ferguson, S. Bhatt, *Report 13: Estimating the number of infections and the impact of non-pharmaceutical interventions on COVID-19 in 11 European countries*, (MRC Centre for Global Infectious Disease Analysis, Imperial College London, 2020).
36. L. J. Wolfson, R. F. Grais, F. J. Luquero, M. E. Birmingham, P. M. Strebel, Estimates of measles case fatality ratios: a comprehensive review of community-based studies. *International journal of epidemiology* **38**, 192-205 (2009).
37. S. Xu, W. Huang, J. Qian, L. Jin, Analysis of genomic admixture in Uyghur and its implication in mapping strategy. *The American Journal of Human Genetics* **82**, 883-894 (2008).
38. C. Fraser, C. A. Donnelly, S. Cauchemez, W. P. Hanage, M. D. Van Kerkhove, T. D. Hollingsworth, J. Griffin, R. F. Baggaley, H. E. Jenkins, E. J. Lyons, Pandemic potential of a strain of influenza A (H1N1): early findings. *Science* **324**, 1557-1561 (2009).
39. F. M. Guerra, S. Bolotin, G. Lim, J. Heffernan, S. L. Deeks, Y. Li, N. S. Crowcroft, The basic reproduction number (R0) of measles: a systematic review. *The Lancet. Infectious diseases* **17**, e420-e428 (2017).
40. J. K. Taubenberger, D. M. Morens, 1918 Influenza: the mother of all pandemics. *Revista Biomedica* **17**, 69-79 (2006).

41. J. Hellewell, S. Abbott, A. Gimma, N. I. Bosse, C. I. Jarvis, T. W. Russell, J. D. Munday, A. J. Kucharski, W. J. Edmunds, F. Sun, Feasibility of controlling COVID-19 outbreaks by isolation of cases and contacts. *The Lancet Global Health* **8**, 488-496 (2020).
42. Coronavirus: Wuhan in first virus cluster since end of lockdown. *BBC*. Retrieved from <https://www.bbc.com/news/world-asia-china-52613138> (2020, May 11).
43. L. Caiyu, City in Jilin declares wartime control mode over COVID-19. *The Global Times*. Retrieved from <https://www.globaltimes.cn/content/1187855.shtml> (2020, May 10).
44. K. Pladson, 1.8 million people in Germany could be infected with coronavirus, researchers find. Retrieved from <https://www.dw.com/en/18-million-people-in-germany-could-be-infected-with-coronavirus-researchers-find/a-53330608> (2020, May 4).